Doping dependence of the electronic Raman spectra in cuprates

F. Venturini[a], M. Opel[a], R. Hackl[a], H. Berger[b], L. Forró[b] and B. Revaz[c]

[a]Walther Meissner Institute, Bavarian Academy of Sciences, D-85748 Garching, Germany

[b]EPFL, Ecublens, CH-1015 Lausanne, Switzerland

[c]DPMC, University of Geneva, CH-1211 Geneva, Switzerland

We report electronic Raman scattering measurements on $Bi_2Sr_2(Y_{1-x}Ca_x)Cu_2O_{8+\delta}$ single crystals at different doping levels. The dependence of the spectra on doping and on incoming photon energy is analyzed for different polarization geometries, in the superconducting and in the normal state. We find the scaling behavior of the superconductivity pair-breaking peak with the carrier concentration to be very different in B_{1g} and B_{2g} geometries. Also, we do not find evidence of any significant variation of the lineshape of the spectra in the overdoped region in both symmetries, while we observe a reduction of the intensity in B_{2g} upon decreasing photon energies. The normal state data are analyzed in terms of the memory-function approach. The quasiparticle relaxation rates in the two symmetries display a dependence on energy and temperature which varies with the doping level.

1. Introduction

Inelastic light-scattering (Raman) experiments reveal a two-particle response of interacting electrons in a similar way as infrared spectroscopy hence combining advantages of angle resolved photoemission spectroscopy (ARPES), by allowing momentum resolution, and of conductivity measurements. Raman studies of the electron properties in cuprates have already been carried out for various doping levels in samples of $Bi_2Sr_2(Y_{1-x}Ca_x)Cu_2O_{8+\delta}$ (Bi-2212), $YBa_2Cu_3O_{6+x}$ (Y-123), and $La_{2-x}Sr_xCuO_4$ (LSCO) [1–4]. However, there are still many unclarified issues as well as considerable improvements in sample quality which motivate a detailed analysis of electronic properties below and above T_c with doping p. In fact, for the understanding of superconductivity in the cuprates the properties of the normal state are considered to be as crucial as those below T_c since the relevant interactions have a characteristic influence on the carriers at all temperatures.

Through the choice of the incident and scattered polarization vectors, Raman scattering is sensitive to different portions of the Fermi surface. By selecting the incident and scattered light polarizations parallel to x and y directions respectively, x and y being parallel to the Cu-O bonds, the B_{2g} symmetry is projected out. In this case the excitations with momenta along the diagonals of the Brillouin zone (BZ) are mainly probed. With polarizations along $x'y'$ (at 45° to the Cu-O bonds) the B_{1g} symmetry is selected. Then the excitation probed are those with momenta along the BZ axes.

In this paper we report electronic Raman scattering measurements in B_{1g} and B_{2g} polarization geometries at different doping levels in the superconducting and in the normal state. For $T > T_c$ the data are analyzed in terms of the memory function approach recently introduced to extract dynamical relaxation rates of the carriers [3].

2. Experiment

High quality $Bi_2Sr_2(Y_{1-x}Ca_x)Cu_2O_{8+\delta}$ single crystals were prepared in ZrO crucibles. They cover a wide doping range as summarized in Table 1. The doping level p is calculated from the relation $T_c = T_c^{max}[1 - 82.6(p - 0.16)^2]$ [5].

The experiments were performed in pseudo back-scattering geometry using a standard Raman setup and an Ar^+ laser for excitation at 458 nm, 514 nm and 528 nm, and a Kr^+ laser at 647 nm. To reduce the heating of the sample due to

Table 1
Bi-2212 single crystals studied.

T_c(K)	57	92	92	78	62	56
p	0.09	0.15	0.16	0.20	0.22	0.23

the absorbed radiation, the power of the laser was maintained below 4 mW. The temperatures given below are corrected for the laser-induced heating as estimated from the ratio of the Stokes to the anti-Stokes intensities. The measured spectra are divided by the Bose-Einstein factor to display the Raman response χ''.

3. Superconducting state

Fig. 1 shows the B_{1g} and B_{2g} electronic Raman spectra in differently doped Bi-2212 samples in the superconducting state at approximately 10 K and in the normal state at approximately 90 K. The data are plotted as a function of energy normalized to the respective transition temperatures of the samples to better visualize the scaling of relevant energies with T_c.

The superconductivity-induced features in B_{1g} and B_{2g} symmetries show a very different scaling behavior with the carrier concentration. We will discuss first the B_{1g} symmetry results. As the carrier concentration decreases from overdoped, Fig. 1(a), to underdoped, Fig. 1(e), the B_{1g} spectrum undergoes substantial modifications. In particular, the intensity is strongly suppressed when reducing the doping level, and for $p < 0.15$ there is no evidence of superconductivity-induced features (Fig. 1(e)), since there is no observable difference between the superconducting and the normal state spectra. The energy of the superconductivity-induced feature ω_{peak}, is also strongly affected by doping, going from $\hbar\omega_{peak}/k_BT_c \sim 4.5$ in the most overdoped sample (Fig. 1(a)) to $\hbar\omega_{peak}/k_BT_c \sim 8.7$ in the slightly underdoped one (Fig. 1(d)). From these observations we conclude that, in the doping range studied, the peak energy is not proportional to k_BT_c but decreases monotonically with increasing p. It is worth noticing that we observe the same doping dependence in Y-123 samples [6].

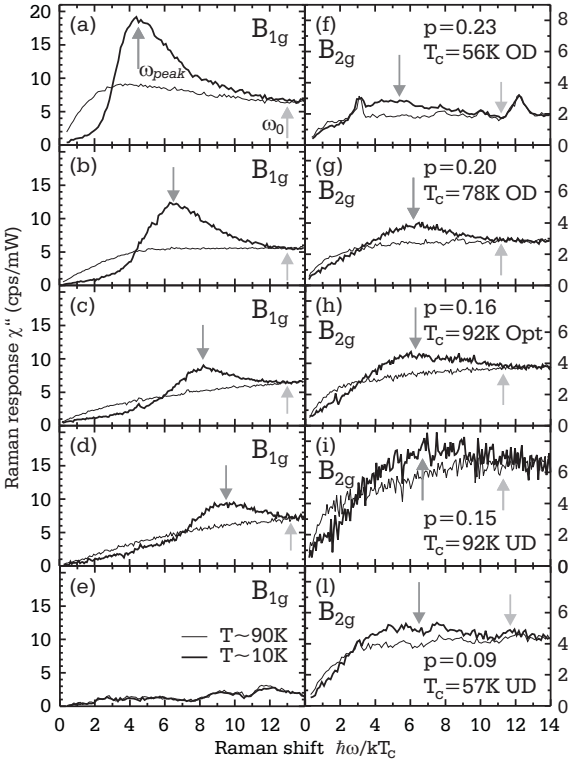

Figure 1. Doping dependence of the Raman spectra in B_{1g} and B_{2g} symmetries in the superconducting and normal state. The arrows mark the ω_{peak} and ω_0 energies.

In contrast, the B_{2g} spectra show a superconductivity-induced feature at all doping levels as it is evident from Fig. 1(f) to Fig. 1(l). In addition, the maxima of the superconducting spectra $\hbar\omega_{peak}/k_BT_c$ are roughly constant between 6 and 6.5, with the exception of the the most overdoped sample (Fig. 1(f)).

Assuming the superconducting gap to vary as $\Delta(\mathbf{k}) = \Delta_0/2\,(\cos(k_x) - \cos(k_y))$, it is possible to extract the maximum Δ_0 [7]. In the B_{2g} symmetry the measured spectra support Δ_0 scaling with T_c. In addition, the effects of superconductivity are observable up to an energy $\hbar\omega_0$ (see Fig. 1), where the superconducting and normal spectra merge, which again scales with T_c, both in B_{1g}

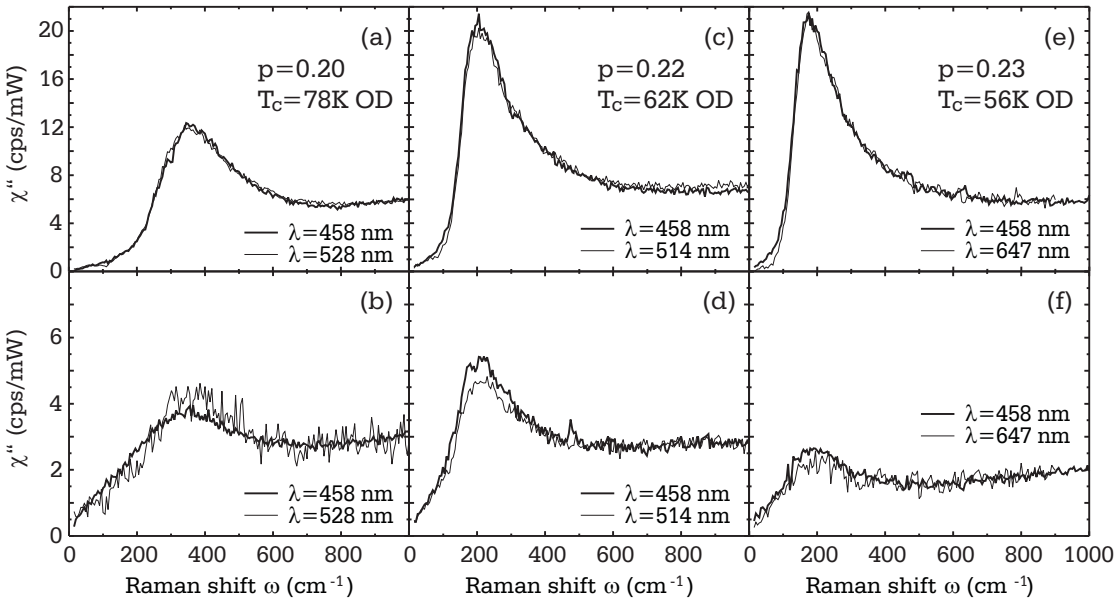

Figure 2. B_{1g} and Raman B_{1g} spectra of overdoped Bi-2212 samples in the superconducting state ($T \sim 10$ K) at different excitation energies as indicated.

and B_{2g} symmetries, at any doping level studied.

The scaling of Δ_0 with T_c is consistent with the results for the superconducting energy gap derived from the magnetic penetration depth [8], electron tunneling for low bias voltages well below the gap [9], as well as Andreev reflection measurement [10]. However, if the B_{1g} peak energy $\hbar\omega_{peak}$ is considered, Raman scattering seems to reveal an additional energy scale which increases monotonically when decreasing the doping level. This can not be explained in the framework of a simple d-wave superconducting energy gap, consistently with the B_{2g} symmetry and requires further theoretical work. In addition, the doping dependence of ω_{peak} resembles that of the energy scale probed by ARPES and tunneling experiments [11,12].

It has been suggested that there are two relevant energy scales, namely the single-particle excitation energy, probed by ARPES and tunneling spectroscopies, which increases by decreasing the doping, and a coherence energy scale, obtained for example by Andreev reflections or B_{2g} Raman scattering [10]. These two energies approach the same value at high doping levels, where the material is believed to recover a BCS-like behavior, and become increasingly different at low dopings. The interpretation of these energy scales and their relation is still an unsolved question. However, to clearly address these questions more experiments are required to investigate the ω_{peak} scaling behavior in the underdoped side of the phase diagram and at which dopings the pair-breaking peak disappears in the B_{1g} symmetry.

In order to further investigate the superconductivity-induced features, we have studied the spectra of the three overdoped Bi-2212 samples at different excitation energies. In fact, it has been previously argued that resonance properties of the pair-breaking excitations are observable in highly overdoped Bi-2212 samples in B_{1g} symmetry, and that they are possibly a signature of an antiferromagnetically correlated Fermi liquid [13].

We analyzed the electronic contribution for excitation energies between 1.6 eV and 2.7 eV in B_{1g}

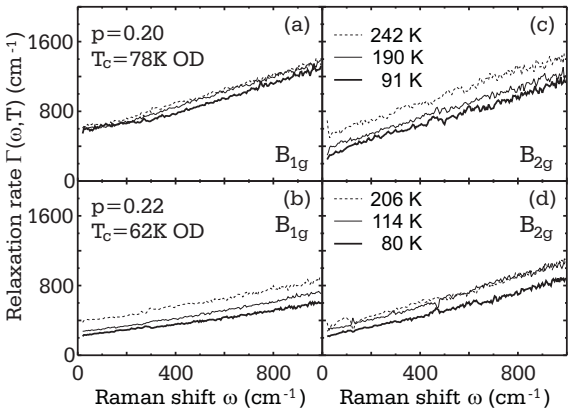

Figure 3. Relaxation rates in B_{1g} ((a),(b)) and B_{2g} ((c),(d)) symmetries at different temperatures for two overdoped samples.

and B_{2g} scattering geometries. Fig. 2 shows the Raman intensity in the B_{1g} and B_{2g} symmetries for three overdoped Bi-2212 samples. In all cases the overall spectra at wavelengths $\lambda \neq 458$ nm have been multiplied by a factor, ranging from 0.7 to 2, to adjust the intensity at 800-1000 cm^{-1} to the spectra at $\lambda = 458$ nm. In both configurations we do not find any significant variation of the lineshape of the spectra with excitation energy at any doping level. However, we observe a reduction of the overall intensity in the B_{2g} symmetry upon decreasing photon energies. Hence, we cannot observe a specific variation of the pair breaking feature with excitation energy neither in Bi-2212 nor in Y-123, except for a small change in the overall cross section.

4. Normal state

The Raman continua in the normal state, $T > T_c$, (see e.g. Fig. 1) contain information on the dynamical two particle lifetime τ for different regions in **k**-space. In Fig. 3 we show the relaxation rates $\Gamma(\omega, T) = 1/\tau$ for two Bi-2212 samples with p=0.20 and p=0.23, derived as described in [3]. The contributions from the phonons have already been subtracted out.

Both in B_{1g}, Fig. 3(a,b), and B_{2g}, Fig. 3(c,d), symmetries, the variation with frequency of the quasiparticle relaxation rates show only little dependence on momentum and doping. As compared to results at lower doping level [3], there is a tendency to a more quadratic frequency dependence below approximately 400 cm^{-1} in the B_{1g} symmetry possibly indicating more conventional quasiparticle dynamics.

The dependence of the dc limit of the relaxation rates $\Gamma_0(T) = \Gamma(\omega \to 0, T)$ on temperature evolves differently with doping in the two symmetries analyzed. In particular, while $\Gamma_0(T)$ decreases with temperature at all doping levels in the B_{2g} symmetry, consistently with ordinary and optical transport [14,15], $\Gamma_0^{B_{1g}}(T)$ is constant or slightly decreasing with T for p=0.20 and assumes the B_{2g} behavior at $p \geq 0.22$. This disappearance of the anisotropy in the small doping range between 0.20 and 0.22 is directly visible in Fig. 3, where the $p = 0.22$ sample shows a strongly suppressed relaxation rate in the B_{1g} symmetry (Fig. 3(b)). We thus believe that the fundamental change in the carrier dynamics close to $(\pi, 0)$ is an intrinsic property of the electron system itself and is closely related to correlation effects which are found to fade away in this doping range in several other experiments [16]. This implies that the underlying interactions, ordering phenomena, and/or fluctuations must have some structure in momentum space.

5. Conclusions

We presented electronic Raman scattering results on Bi-2212. In the SC state, the B_{1g} and B_{2g} symmetry spectra are characterized by very different doping dependences of the superconductivity-induced features. While the B_{2g} spectra are consistent with a superconducting energy gap with d-wave symmetry and a maximum Δ_0 scaling with T_c, the B_{1g} symmetry requires further theoretical work. In the normal state the quasiparticles at $(\pi, 0)$ and at $(\pi/2, \pi/2)$ are characterized by a qualitatively different doping dependence of the relaxation rates. At high doping levels, $p \geq 0.22$, the anisotropy observed for $p \leq 0.20$seems to disappear.

F.V. would like to thank the Gottlieb Daimler and Karl Benz Foundation for financial support.

REFERENCES

1. C. Kendziora and A. Rosenberg, Phys. Rev. B **52**, 9867 (1995).
2. X.K. Chen *et al.*, Phys. Rev. B **56**, R513 (1997); J. Naeini *et al.*, Phys. Rev. B **59**, 9642 (1999).
3. M. Opel *et al.*, Phys. Rev. B **61**, 9752 (2000).
4. S. Sugai and T. Hosokawa, Phys. Rev. Lett. **85**, 1112 (2000).
5. J.L. Tallon *et al.*, Phys. Rev. B **51**, 12911 (1995).
6. R. Nemetschek *et al.*, Eur. Phys. J. B **5**, 495 (1998)
7. T.P. Devereaux and D. Einzel, Phys. Rev. B **51**, 16336 (1995).
8. C. Panapogoulos *et al.*, Phys. Rev. B **57**, 13422 (1998).
9. C. Renner *et al.*, Phys. Rev. Lett. **80**, 149 (1998).
10. G. Deutscher, Nature **397**, 410 (1999).
11. N. Miyakawa *et al.*, Phys. Rev. Lett. **80**, 157 (1998).
12. J. Mesot *et al.*, Phys. Rev. Lett. **83**, 840 (1999).
13. M. Rübhausen *et al.*, Phys. Rev. Lett. **82**, 5349 (1999).
14. D.B. Tanner and T. Timusk, in Physical Properties of High-Temperature Superconductors III, ed. by D.M. Ginzberg (World Scientifi, Singapore, 1992)
15. C. Kendziora *et al.*, Phys. Rev. B **48**, 3531 (1993).
16. J.L. Tallon ans J.W Loram, Physica C **349**, 53 (2001).